iScience

CellPress
OPEN ACCESS

Article

IGFBP3 promotes resistance to Olaparib via modulating EGFR signaling in advanced prostate cancer

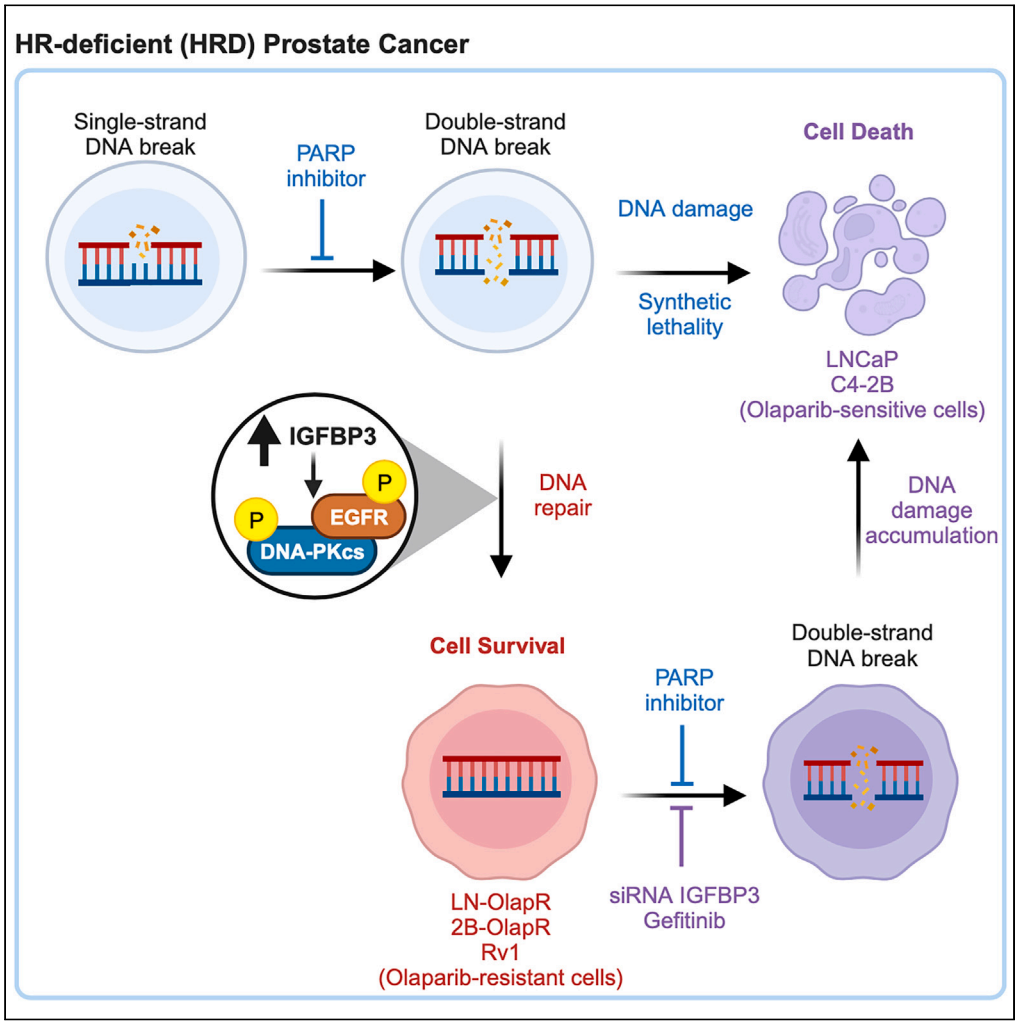

Amy R. Leslie, Shu Ning, Cameron M. Armstrong, ..., Christopher P. Evans, Alan P. Lombard, Allen C. Gao

acgao@ucdavis.edu

Highlights

IGFBP3 is highly expressed in Olaparib-resistant advanced prostate cancer (PC)

IGFBP3 inhibition restored Olaparib sensitivity in resistant, acquired and intrinsic, PC

IGFBP3 drives Olaparib resistance through the EGFR/DNA-PKcs pathway

EGFR small molecule inhibitor, Gefitinib, synergizes with Olaparib and depleted cell growth

Leslie et al., iScience 27, 108984
February 16, 2024
https://doi.org/10.1016/j.isci.2024.108984

iScience

CellPress
OPEN ACCESS

Article

IGFBP3 promotes resistance to Olaparib via modulating EGFR signaling in advanced prostate cancer

Amy R. Leslie,[1] Shu Ning,[1] Cameron M. Armstrong,[1] Leandro S. D'Abronzo,[1] Masuda Sharifi,[1] Zachary A. Schaaf,[1] Wei Lou,[1] Chengfei Liu,[1,2] Christopher P. Evans,[1,2] Alan P. Lombard,[1,3] and Allen C. Gao[1,2,4,5,*]

SUMMARY

Olaparib is a pioneering PARP inhibitor (PARPi) approved for treating castration-resistant prostate cancer (CRPC) tumors harboring DNA repair defects, but clinical resistance has been documented. To study acquired resistance, we developed Olaparib-resistant (OlapR) cell lines through chronic Olaparib treatment of LNCaP and C4-2B cell lines. Here, we found that IGFBP3 is highly expressed in acquired (OlapR) and intrinsic (Rv1) models of Olaparib resistance. We show that IGFBP3 expression promotes Olaparib resistance by enhancing DNA repair capacity through activation of EGFR and DNA-PKcs. IGFBP3 depletion enhances efficacy of Olaparib by promoting DNA damage accumulation and subsequently, cell death in resistant models. Mechanistically, we show that silencing IGFBP3 or EGFR expression reduces cell viability and resensitizes OlapR cells to Olaparib treatment. Inhibition of EGFR by Gefitinib suppressed growth of OlapR cells and improved Olaparib sensitivity, thereby phenocopying IGFBP3 inhibition. Collectively, our results highlight IGFBP3 and EGFR as critical mediators of Olaparib resistance.

INTRODUCTION

The progression of therapeutic resistance continues to be one of the biggest challenges in prostate cancers.[1] The androgen receptor (AR) signaling pathway is crucial for all stages of prostate cancer.[2,3] Androgen deprivation therapy (ADT) is the golden standard for treating prostate cancer.[4] Many patients will respond to ADT, but eventually the incurable disease will tolerate drug therapeutics.[5,6] Tumors acquire mutations that allow these malicious cancer cells to overcome anticancer therapy through diverse escape mechanisms, thus evolving into castration-resistant prostate cancer (CRPC).[7] The next-generation anti-androgen therapies (NGATs) were developed to treat CRPC, which has greatly improved patient survivability.[8–10] Alas, CRPC patients eventually relapse as the tumors prevail against AR-targeted therapies.[11–13]

Poly(ADP-ribose) polymerase inhibitors (PARPi) are a revolutionary class of targeted therapeutics that weaponizes the tumor cell's homologous recombination (HR) defects by disrupting PARP's function to repair DNA breaks.[14,15] This approach selectively kills tumor cells with HR defects while sparing the patient's nonmalignant cells, in a process termed synthetic lethality.[16] The landmark battles of 2005 discovered that epithelial cancers lacking germline BRCA1, BRCA2, and ATM struggle to repair double-strand DNA breaks (DSBs) due to the cancer cell's inability to perform homology-directed DNA repair, thus are vulnerable to DNA damage.[17–19] Members of the poly(ADP-ribose) polymerase (PARP) family have a highly conserved ADP-ribosyl transferase (ART) domain and are involved in many cellular pathways that regulate genomic DNA integrity.[20] PARP1 and PARP2 are the only DNA-dependent PARPs required to facilitate the repair of both single-strand and double-strand breaks through their conserved Tyr-Gly-Arg (WGR) domain.[21] Thus, PARPi's will induce DNA damage and trigger cell death in tumor cells which lack adequate capacity to repair DNA damage.

Metastatic CRPC can develop genomic mutations that interfere with DNA repair.[22–24] The *BRCA* genes are the most frequently mutated DNA damage response (DDR) gene in prostate cancer and are responsible for genomic integrity maintenance through HR pathway.[17,25] Patients with metastatic CRPC are prone to higher incidences of germline mutations in DRR genes compared to primary prostate cancer, thus genomic integrity is compromised.[26–29] Metastatic prostate cancer afflicted with DDR genomic aberrations have a favorable response to PARP inhibitors due to this HR vulnerability caused by the destabilized genome.[23] The phase III PROfound trial granted the PARP inhibitor, Olaparib, breakthrough therapy designation which prompted the Food and Drug Administration (FDA) to approve Olaparib for the treatment of metastatic CRPC (mCRPC).[22] About 20% of mCRPC patients have mutations in HR genes such as BRCA1, BRCA2, and ATM.[30,31] However, the drugs used to treat mCRPC patients carrying HR mutations impose selective pressure which leads to the formation of PARPi resistance.[32]

[1]Department of Urologic Surgery, University of California Davis, Davis, CA, USA
[2]UC Davis Comprehensive Cancer Center, University of California Davis, Davis, CA, USA
[3]Department of Biochemistry and Molecular Medicine, University of California Davis, Davis, CA, USA
[4]VA Northern California Health Care System, Sacramento, CA, USA
[5]Lead contact
*Correspondence: acgao@ucdavis.edu
https://doi.org/10.1016/j.isci.2024.108984

Despite the clinical effectiveness of PARPi's, resistance in advanced stages of prostate cancer has been observed in which tumor cells restore their HR repair (HRR) capacity.[33,34] The mechanisms underlying the development of resistance are largely unknown. Reversion mutations are one scenario in which clinically documented PARPi resistant tumors regain BRCA1 or BRCA2 functions and are no longer deficient in HR genes.[35,36] We have previously developed Olaparib-resistant (OlapR) prostate cancer cells and characterized their response to Olaparib to elucidate the underlying mechanisms of PARPi resistance.[37] The OlapR cells are highly resistant toward Olaparib, and in fact, show cross-resistance toward several PARPi's including but not limited to Rucaparib, Talazoparib, and Niraparib. It was discovered, that unlike their sensitized counterparts, the OlapR cells fail to arrest the G2/M checkpoint and display a blunted response to Olaparib. Interestingly, the OlapR models exhibit increased DNA damage which suggests that the mechanism of resistance stems from DSB repair pathways.[37] Repairing DSBs requires the phosphorylation of histone H2AX at serine 139, forming γH2AX, which initiates the recruitment of the DNA damage response (DDR).[38] The activation of γH2AX serves as a checkpoint for HR and NHEJ repair pathways.[39] The HR pathway represents a high-fidelity repair process, while the NHEJ pathway is intrinsically mutagenic.[40] During the cell cycle, HR is restricted to S/G2 phase following DNA replication whereas NHEJ has free reign.[41] Biochemical analysis of post-translational modifications reveals increased γH2AX in the OlapR cells which suggests that the mechanism behind PARPi resistance depends on their ability to endure persistent DNA damage.

Previous studies have found that the overexpression of IGFBP3 is a strong predicator of prostate cancer progression, tumor recurrence, and poor patient survival.[42] IGFBP3 plays a major role in the DDR. Specifically, IGFBP3 plays an active role in the NHEJ repair pathway.[43] During NHEJ, the catalytic subunit of DNAPK (DNAPKcs) along with the Ku70/80 heterodimer is necessary for repairing DSBs.[44] It has been demonstrated that exogenous DNA damage induces autophosphorylation of DNAPKcs at serine 2056 in breast cancer models.[45] Furthermore, IGFBP3 was found to potentiate epidermal growth factor (EGF) signaling to stimulate EGF receptor (EGFR) activation, which modulates NHEJ DSB repair by forming a complex with DNAPKcs.[45–47]

In this study, we found that IGFBP3 is overexpressed in OlapR cells. We examined the effects of IGFBP3 on Olaparib resistance and DNA damage. We uncovered DNA repair response strategies employed to re-sensitize PARPi resistant tumors and thus, circumvent drug resistance mediated by overexpression of IGFBP3 and activation of EGFR signaling. We showed that IGFBP3 and EGFR are highly upregulated in the OlapR models. IGFBP3 depletion in OlapR cells reduces the phosphorylation of DNAPKcs. With IGFBP3 knockdown, the resistant models increase DNA damage and exhibit Olaparib sensitivity. Treatment with a combination of PARP and EGFR inhibitors resulted in synergistic growth inhibition of OlapR cells, implicating IGFBP3-EGFR signaling as a mediator of resistance to PARP1-targeting agents. These findings propose that upregulation of IGFBP3 promotes Olaparib resistance by enhancing the formation of the IGFBP3/EGFR/DNAPKcs protein complex in response to DNA damage, thus overcoming the effects of Olaparib. Our results suggest that combining PARPi's with other DDR target inhibitors like Gefitinib may have therapeutic advantages in certain CRPC subtypes and warrants further investigation.

RESULTS

IGFBP3 is highly expressed in models of Olaparib resistance

In our previous studies, we have generated two Olaparib-resistant (OlapR) cell sublines named LN-OlapR and 2B-OlapR from LNCaP and C4-2B cells, respectively.[37] The OlapR models are far less sensitizing to Olaparib than the parental cells.[37] Olaparib significantly inhibits the proliferation of LNCaP and C4-2B parental cells but has little effect on their resistant derivatives (Figures S1A and S1B). LNCaP is representative of castration-sensitive prostate cancer cells while C4-2B is representative of CRPC cells. LNCaP and C4-2B cell lines are excellent preclinical models to study CRPC progression.[48] LNCaP has BRCA2 mutations while C4-2B cells are derived from LNCaP-derived, castration-resistant C4-2 cells.[49] LNCaP cells feature other HR mutations in RAD51B, RAD54L, ATM, and FANCA, which supports the argument that extreme HR vulnerability contributes to Olaparib sensitivity.[24,50,51] Thus, providing the rationale that LNCaP and C4-2B would exhibit Olaparib sensitivity.

To understand potential mechanisms underlying resistance to Olaparib, we employed transcriptomics to analyze alterations in pathways in OlapR resistant models. RNA-seq analyses in OlapR models identified 455 upregulated genes conserved between LN-OlapR and 2B-OlapR (Figure 1A). Specifically, the transcriptomics profiling revealed that IGFBP3 is highly expressed in the resistant cells (Figures 1B, S1C, and S1D) and validated the increased IGFBP3 mRNA levels by qPCR (Figure 1C). IGFBP3 has been identified as a biomarker for treatment resistance in advanced stages of prostate cancer.[42,47,52] In addition, IGFBP3 overexpression is strongly associated with clinical tumor aggressiveness, prostate cancer recurrence after ADT, and poor prognosis.[42,47,53] IGFBP3 is significantly upregulated in high Gleason score prostate cancer patients in TCGA and DKFZ datasets (Figure 1D).

To assess IGFBP3 expression levels in OlapR cells, we performed western blot analyses. The results show that IGFBP3 expression is significantly increased at the protein level in LN-OlapR and 2B-OlapR cells (Figure 1E). IGFBP3 contains both a 27 amino acid signal peptide at the N-terminus and a nuclear localization signal at the C-terminus, which allows for IGFBP3 extracellular secretion and nuclear transportation, respectively.[54] This secretory signal peptide sequence allows for the extracellularly secretion of IGFBP3.[55] To assess the secretion of IGFBP3 in the OlapR models, we measured the concentration of IGFBP3 in the culture medium supernatant using an ELISA assay. We found that IGFBP3 secretion is increased in the resistant models compared to the parental cells (Figure 1F). Collectively, our findings support that high levels of IGFBP3 are indicative of Olaparib resistance.

Olaparib induces DNA damage and ensuing apoptosis in cancer cells harboring DNA repair defects.[23] Olaparib-treated LNCaP and C4-2B cells exhibit increased γH2AX (Figure 1G), but the OlapR cells have no increase in γH2AX levels when treated with Olaparib.[37] In LNCaP and C4-2B cells treated with Olaparib, there is an increase in IGFBP3 mRNA and protein levels which coincides with the increased γH2AX thus revealing the connection between IGFBP3 and DSB repair pathways (Figures 1G and 1H). This finding is consistent with OlapR models, LN-OlapR and 2B-OlapR, having significantly higher levels of γH2AX compared to their parental counterparts, LNCaP and C4-2B, by western

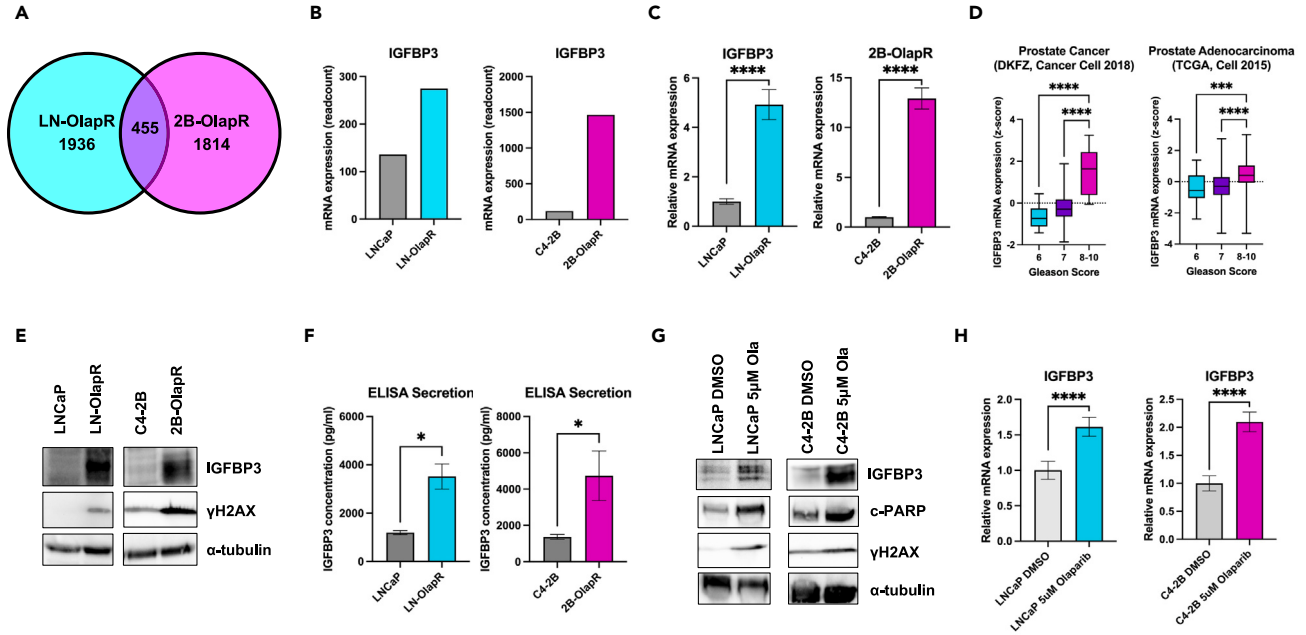

Figure 1. IGFBP3 is highly expressed in Olaparib-resistant LN-OlapR and 2B-OlapR cell line models

(A) Venn diagrams of RNA-sequencing analysis of LN-OlapR and 2B-OlapR depicting the upregulated genes (minimum 2-fold change).

(B) The mRNA expression levels of IGFBP3 in LN-OlapR and 2B-OlapR cells were determined by RNAseq (read count).

(C) Relative mRNA expression levels of IGFBP3 in LN-OlapR and 2B-OlapR cells were determined by qPCR.

(D) In two cBioPortal databases (DKFZ and TCGA), IGFBP3 gene expression levels were determined in tumor samples of different Gleason scores.

(E) The protein expression of IGFBP3 and γH2AX in parental cells, OlapR cells was determined by western blot analysis. Tubulin served as a loading control.

(F) The secretion of IGFBP3 was determined by ELISA between OlapR and parental cell line.

(G) The protein expression of c-PARP and γH2AX in LNCaP and C4-2B cells treated with 5μM Olaparib or vehicle control for two days was determined by western blot analysis. Tubulin served as a loading control.

(H) Relative mRNA expression levels of IGFBP3 in LNCaP and C4-2B cells treated with 5μM Olaparib or vehicle control for 48 h were determined by qPCR. p value less than 0.05 was considered significant (*, $p < 0.05$; **, $p < 0.01$; ***, $p < 0.001$; ****, $p < 0.0001$). Statistical analysis was performed using Student's t test and one-way ANOVA.

blot analysis (Figure 1E). The high levels of γH2AX confirm the presence of DNA damage in the resistant models and indicate activation of the DSB repair pathways, which includes HR and NHEJ. Thus, Olaparib treatment recruits IGFBP3 to respond to DNA damage in the sensitive setting. These results suggest that IGFBP3 overexpression augments DSB repair to promote Olaparib resistance.

IGFBP3 inhibition reduces cell growth and enhances Olaparib sensitivity

To test whether IGFBP3 affects Olaparib resistance in OlapR models, we performed cell growth assays using small interfering RNA (siRNA)-mediated IGFBP3 knockdown. We found that silencing IGFBP3 decreases IGFBP3 mRNA and protein levels in OlapR cells using qPCR and western blots (Figures 2A and 2B). Our biochemical assays revealed that IGFBP3 depletion significantly increases γH2AX and cleaved-PARP protein levels in the OlapR models (Figure 2B). This data suggests that the knockdown of IGFBP3 induces DNA damage and apoptosis. OlapR cells treated with IGFBP3 knockdown drastically reduce cell viability (Figure 2C). We next evaluated the effect of siRNA-induced depletion of IGFBP3 on Olaparib sensitivity in the resistant cells (Figures 2D and S2). The cell growth assay suggests that IGFBP3 knockdown enhances the efficiency of Olaparib in the resistant models (Figure 2D), which is accompanied with increased γH2AX and cleaved-PARP expression (Figure 2E). Together, these results demonstrate that IGFBP3 knockdown aids in Olaparib sensitivity in the resistant setting.

EGFR-DNAPKcs signaling is overexpressed in OlapR cells

IGFBP3 has been shown to be involved in DNA repair pathways.[43] IGFBP3 enhances growth factor signaling, leading to ligand-triggered EGFR dimerization. This results in the phosphorylation of EGFR, causing its relocation to the nucleus. Subsequently, this initiates the auto-phosphorylation of the DNAPKcs at the Ser2056 site, an essential step for DNA double-strand break repair through the NHEJ pathway.[44–47] EGFR is a member of the DRR, meaning that DNA damage recruits EGFR, which in turn causes EGFR to mediate its downstream signaling pathways to contribute to DNA repair capacity.[56,57] Using western blot analyses, we found that EGFR phosphorylation levels are increased in both OlapR models (Figure 3A). Additional studies demonstrate that adding recombinant IGFBP3 to 2B-OlapR cells enhances EGFR phosphorylation (Figure S3A), and inhibiting IGFBP3 decreases EGFR phosphorylation but adding EGF ligand elicits EGFR phosphorylation

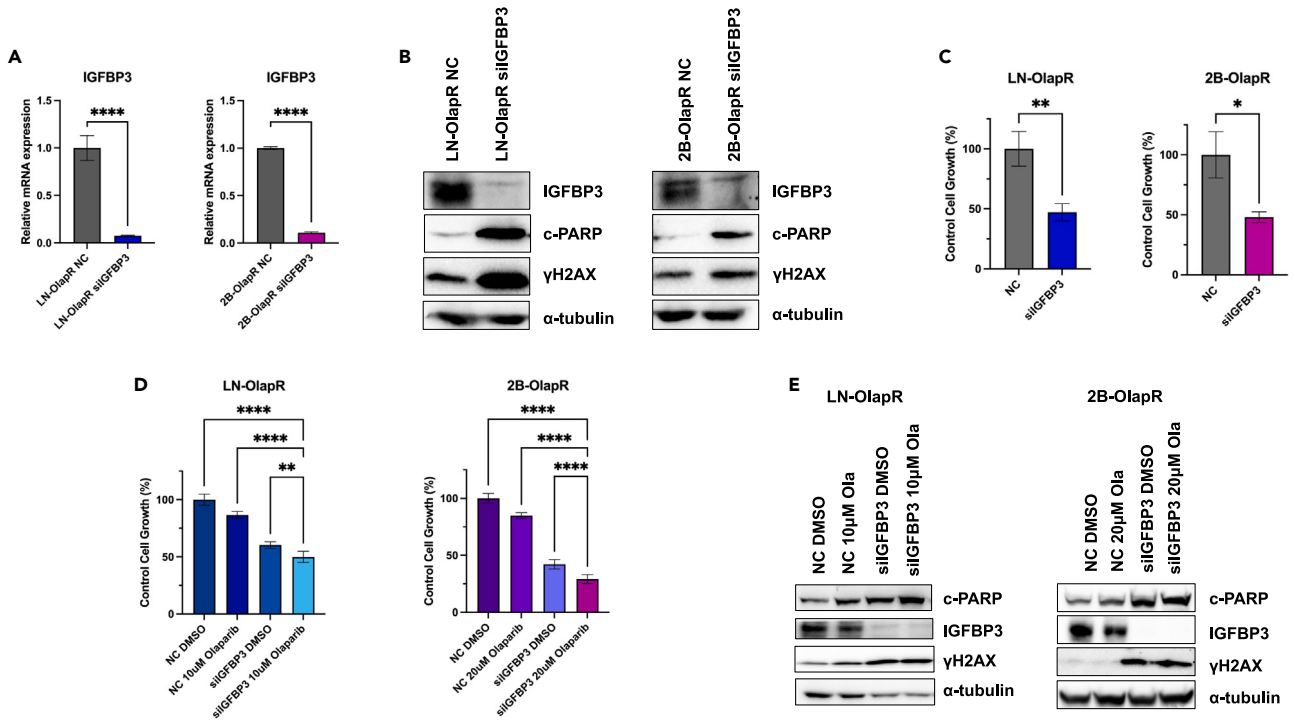

Figure 2. IGFBP3 inhibition induces DNA damage and sensitizes resistant cells to Olaparib treatment

(A) Relative mRNA expression levels of IGFBP3 in LN-OlapR and 2B-OlapR cells after transfection with siRNA targeting IGFBP3 for 48 h were determined by qPCR.

(B) The protein expression of IGFBP3, c-PARP, and γH2AX in LN-OlapR and 2B-OlapR cells treated with siIGFBP3 for 48 h was determined by western blot analysis. Tubulin served as a loading control.

(C) The cell growth of LN-OlapR and 2B-OlapR cells treated with siIGFBP3 for 48 h was determined by CCK-8.

(D) The cell growth of LN-OlapR and 2B-OlapR cells transiently transfected with IGFBP3 siRNA and then treated with Olaparib for 72 h was determined by CCK-8.

(E) The protein expression of IGFBP3, c-PARP, and γH2AX in LN-OlapR and 2B-OlapR cells transiently transfected with IGFBP3 siRNA and then treated with Olaparib for 72 h was determined by western blot analysis. Tubulin served as a loading control. p value less than 0.05 was considered significant (*, $p < 0.05$; **, $p < 0.01$; ***, $p < 0.001$; ****, $p < 0.0001$). Statistical analysis was performed using Student's t test and one-way ANOVA.

(Figure S3B). Furthermore, the levels of DNAPKcs phosphorylation are also upregulated in the OlapR models (Figure 3B). We also found that siRNA mediates depletion of EGFR and decreases cell viability of the 2B-OlapR cells (Figure 3C). These findings suggest that the interaction between both IGFBP3 and EGFR is required for Olaparib resistance by promoting DNA repair mediated by DNAPKcs activation in the resistant setting. EGFR is highly expressed and activated in many cancers and is correlated with poor prognosis.[58] In prostate cancer, EGFR overexpression is associated with prostate cancer metastasis.[59] Data analysis indicates that EGFR and DNAPKcs are significantly upregulated in patients with high Gleason score prostate cancer, respectively (Figures 3D and 3E) (Figure S4).

EGFR inhibition suppresses OlapR cell growth and enhances Olaparib sensitivity

Targeting the function of IGFBP3 may serve as a therapeutic model for sensitizing resistant cells to Olaparib. However, a problem is that IGFBP3 does not have a small molecule inhibitor available. Having demonstrated that inhibition of EGFR by siRNA suppressed growth in 2B-OlapR cells, we decided to target EGFR using pharmacological inhibitors to test if the combination enhances Olaparib sensitivity and phenocopies IGFBP3 inhibition. Using cell growth assays, we demonstrated that treating the OlapR models with the small molecule inhibitor, Gefitinib, targeting EGFR signaling significantly inhibited the growth of OlapR cells (Figures S5A and S5B). Gefitinib inhibited the growth of both OlapR cells in a dose-dependent manner with the IC_{50} values for LN-OlapR = 20.77μmol/L and 2B-OlapR = 17.13μmol/L, respectively (Figure 4A). Using clonogenic assays, we demonstrated that treating Olaparib-sensitive, castration-resistant C4-2B cells and Olaparib-resistant, castration-resistant 2B-OlapR cells with 20μM Gefitinib decreased cell survival (Figures S5C and S5D). Inhibition of EGFR by Gefitinib decreased phosphorylated EGFR protein levels (Figure 4B).

Since IGFBP3 inhibition re-sensitizes the resistant models to Olaparib inhibition, will EGFR inhibition also re-sensitize the OlapR cells to Olaparib treatment? We next test if Gefitinib can improve Olaparib efficacy within the OlapR models. Using cell growth assays, we found that the combination of Olaparib and Gefitinib synergistically inhibited cell growth of the OlapR cells (Figure 4C), indicating that treating the OlapR cells with Olaparib and Gefitinib resensitizes the resistant cells to Olaparib with the combination drug index (CDI) values were less than 0.7 which indicates synergism between the two drugs.[60] In line with the cell growth assay results, the colony formation assays support

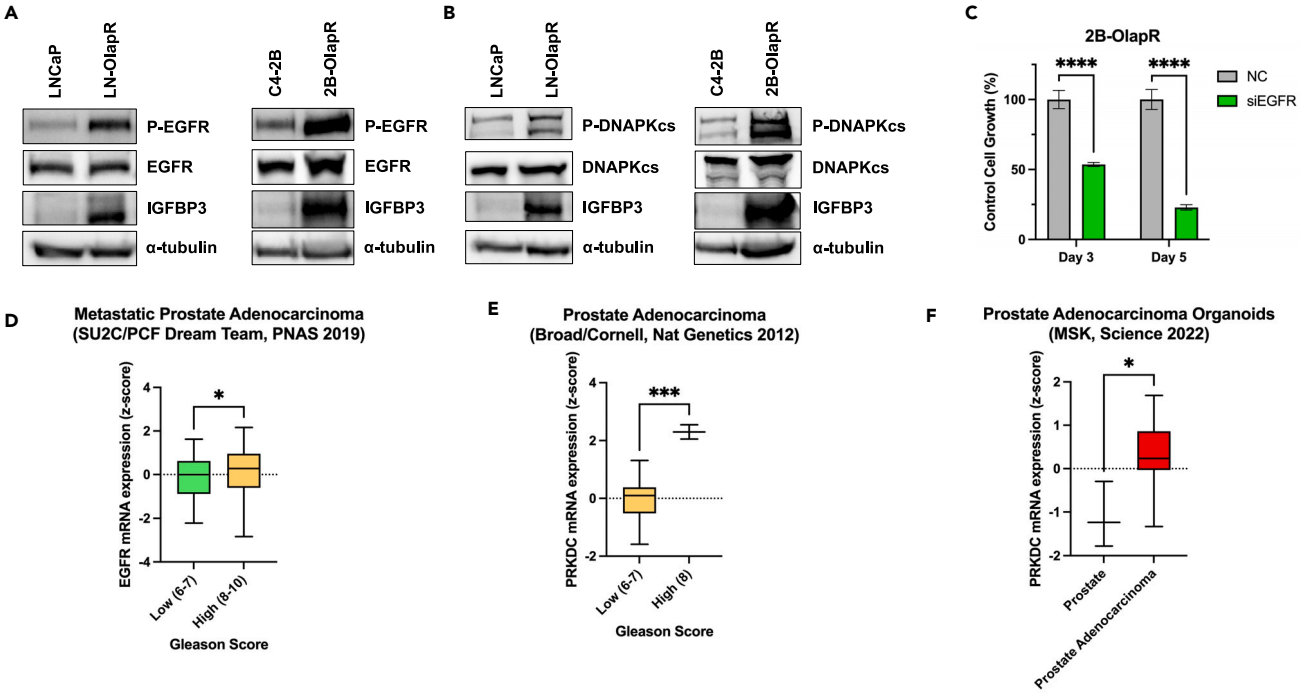

Figure 3. EGFR/DNAPKcs-mediated DSB NHEJ signaling upregulated in Olaparib-resistant prostate cancer

(A) The protein expression of phospho-EGF receptor (Tyr1068) and IGFBP3 in parental cells, OlapR cells was determined by western blot analysis. Tubulin served as a loading control.

(B) The protein expression of phospho-DNA-PKcs (Ser2056) and IGFBP3 in parental cells, OlapR cells was determined by western blot analysis. Tubulin served as a loading control.

(C) The cell growth of 2B-OlapR cells transfected with EGFR siRNA for 3 days and 5 days was determined by CCK-8.

(D) In the cBioPortal database (SUC2/PCF Dream Team, PNAS 2019), EGFR gene expression levels were determined in tumor samples of different Gleason scores.

(E) In the cBioPortal database (Broad/Cornell, Nat Genetics 2012), PRKDC (DNA-PKcs) gene expression levels were determined in tumor samples of different Gleason scores.

(F) In the cBioPortal database (MSK, Science 2022), PRKDC (DNA-PKcs) gene expression levels were determined in organoid derived cancer types, prostate adenocarcinoma and prostate. p value less than 0.05 was considered significant (*, $p < 0.05$; **, $p < 0.01$; ***, $p < 0.001$; ****, $p < 0.0001$). Statistical analysis was performed using Student's t test.

the combination of Olaparib and Gefitinib which showed dramatic inhibition of cell survival in the OlapR models (Figure S6). Lastly, we tested the drug combination in spheroids derived from the 2B-OlapR cell lines which models the unique 3D architecture of tumors. We found that Olaparib and Gefitinib significantly inhibit the 2B-OlapR spheroid cell viability (Figure 4D). The Isobologram analysis also showed that combination of Olaparib and Gefitinib synergistically inhibited cell growth in 2B-OlapR cells[61] (Figure 5). These experiments reveal that Gefitinib alters Olaparib sensitivity and phenocopies IGFBP3 inhibition.

IGFBP3 is overexpressed in Rv1 cells

Acquired and intrinsic are forms of therapeutic resistance.[62] LN-OlapR and 2B-OlapR cell lines serve as models of acquired Olaparib resistance.[37] Rv1 is a castration-resistant, AR-positive human prostate cancer cell line.[63] Despite harboring BRCA2 mutations, suggesting potential sensitivity to PARPi, Rv1 cells demonstrate strong resistance to Olaparib (Figure 6A). This positions the Rv1 cell line as a model for intrinsic Olaparib resistance.[49] We test if IGFBP3 overexpression is associated with the intrinsic Olaparib resistance in Rv1 cells. IGFBP3 is significantly upregulated in Rv1 cells compared to LNCaP and C4-2B cells, respectively (Figure 6B). The Rv1 cells have increased protein levels in P-EGFR and γH2AX compared to LNCaP and C4-2B cells (Figure 6C). Similar to the OlapR models, Rv1 cells also exhibit increased P-DNAPKcs expression (Figure 6D). These experiments support that high levels of IGFBP3 are indicative of Olaparib resistance, both acquirable and intrinsically.

We next tested if IGFBP3 is necessary for intrinsic Olaparib resistance in Rv1 cells. Using a cell growth assay, we found that IGFBP3 inhibition decreases Rv1 cell proliferation (Figure S7A). We confirmed the depletion of IGFBP3 RNA and protein levels in the Rv1 cells (Figures S7B and S7C). As Rv1 cells express high levels of P-EGFR, we examined the effect of increasing doses of Gefitinib on cell growth. Gefitinib inhibits Rv1 cell growth with the IC_{50} value = 13.63 μmol/L (Figures 6E and S7D). Lastly, we treated the Rv1 cells with the Olaparib/Gefitinib combination and found that it synergistically decreases the cell growth and cell survival (Figures 6F and S7E). These results indicate that targeting IGFBP3 and EGFR will impact both acquired and intrinsic Olaparib resistance.

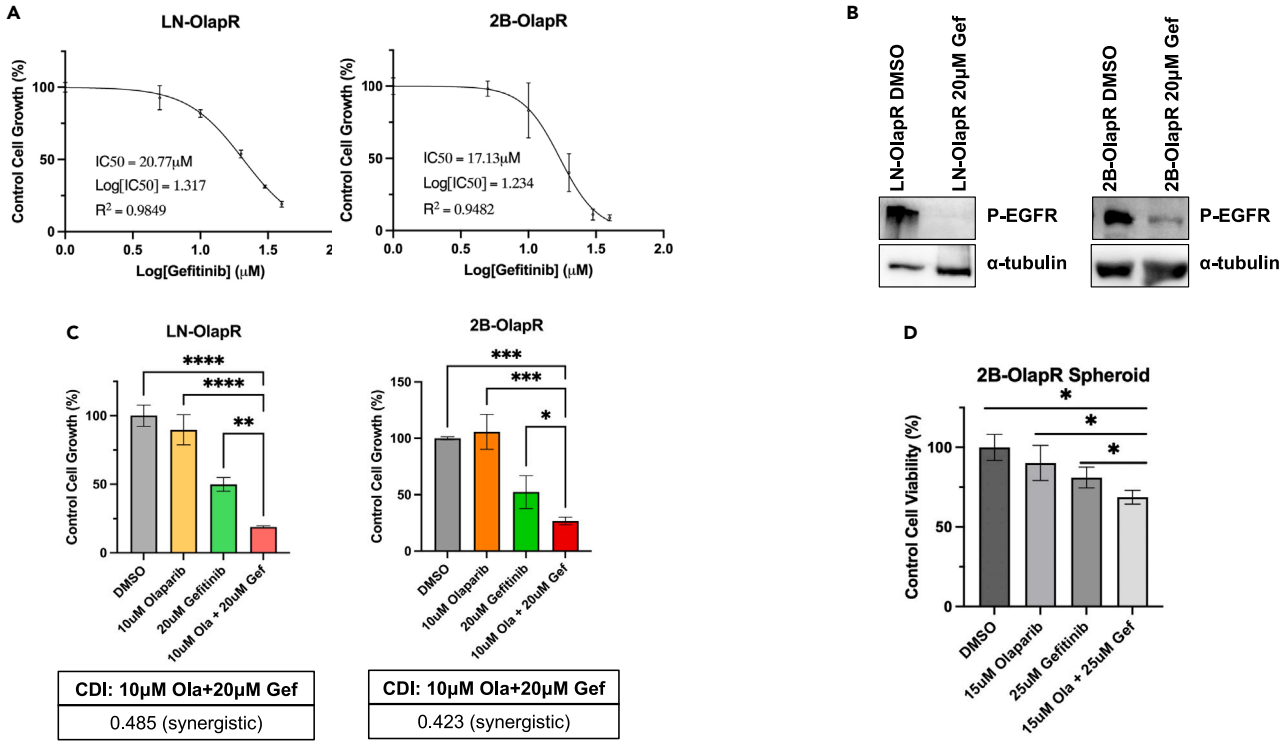

Figure 4. EGFR inhibition and Gefitinib inhibits OlapR cell growth and enhances Olaparib sensitivity

(A) The IC50 values of LN-OlapR and 2B-OlapR treated with Gefitinib via cell growth were determined by CCK-8.

(B) The protein expression of phospho-EGF receptor (Tyr1068) in LN-OlapR and 2B-OlapR cells treated with 20μM Gefitinib for 48 h was determined by western blot analysis. Tubulin served as a loading control.

(C) The cell growth of LN-OlapR and 2B-OlapR treated with 10μM Olaparib and 20μM Gefitinib for 72 h was determined by CCK-8. The combination drug index (CDI) of Olaparib and Gefitinib in LN-OlapR and 2B-OlapR was calculated.

(D) The cell viability of 2B-OlapR derived spheroids treated with 15μM Olaparib and 25μM Gefitinib were determined by Cell Titer Glo. p value less than 0.05 was considered significant (*, $p < 0.05$; **, $p < 0.01$; ***, $p < 0.001$; ****, $p < 0.0001$). Statistical analysis was performed using Student's t test.

DISCUSSION

In this study, we identified a potential mechanism of resistance to the PARP inhibitor Olaparib that involves overexpression of IGFBP3 and activation of EGFR-DNAPKcs pathway in advanced prostate cancer. We found that IGFBP3 is significantly overexpressed in two Olaparib-resistant cell models (LN-OlapR and 2B-OlapR), linked to both acquired and intrinsic resistance. IGFBP3 inhibition via small interfering RNA decreased cell viability and increased sensitivity to Olaparib. We also found that IGFBP3 activates the EGFR-DNAPKcs axis, which is critical for DNA double-strand break repair. We further demonstrate that inhibiting EGFR using Gefitinib decreased cell growth and restored Olaparib sensitivity in the resistant models. Our results indicate that IGFBP3 overexpression and EGFR-DNAPKcs pathway activation play a key role in Olaparib resistance. Targeting IGFBP3 and EGFR could potentially enhance Olaparib's effectiveness in prostate cancer treatment. The Olaparib-resistant (OlapR) sublines, LN-OlapR and 2B-OlapR, display significantly reduced sensitivity to Olaparib compared to their parental LNCaP and C4-2B cells. LNCaP and C4-2B cells harboring homologous recombination (HR) mutations were anticipated to exhibit Olaparib sensitivity, hence the development of resistance warranted investigation. Our exploration into the OlapR resistance mechanisms via transcriptomics revealed that IGFBP3 was markedly overexpressed in resistant OlapR cells. Prior studies indicated that IGFBP3 overexpression was linked with clinical tumor aggressiveness, cancer recurrence post-ADT, and poor prognosis.[42,43,47] This correlation was also validated in high Gleason score prostate cancer patients.[64] Further analyses demonstrated elevated IGFBP3 protein levels in the resistant cell models. The ability of IGFBP3 to be secreted extracellularly, due to its unique structure containing a signal peptide sequence, was also observed in the OlapR models.

To investigate the necessity of IGFBP3 in Olaparib resistance, we knocked down IGFBP3 expression via siRNA and observed a reduction in both mRNA and protein levels of IGFBP3 in Olaparib-resistant (OlapR) cells. We found that IGFBP3 depletion triggered an elevation in γH2AX and cleaved-PARP protein levels in OlapR models, signifying the induction of DNA damage and apoptosis. IGFBP3 knockdown caused a substantial reduction in the viability of OlapR cells. Furthermore, the cell growth assays demonstrated that IGFBP3 knockdown enhanced the efficacy of Olaparib in the resistant models, an effect that was accompanied by increased γH2AX and cleaved-PARP expression. These results offer compelling evidence that IGFBP3 plays a pivotal role in facilitating Olaparib resistance.

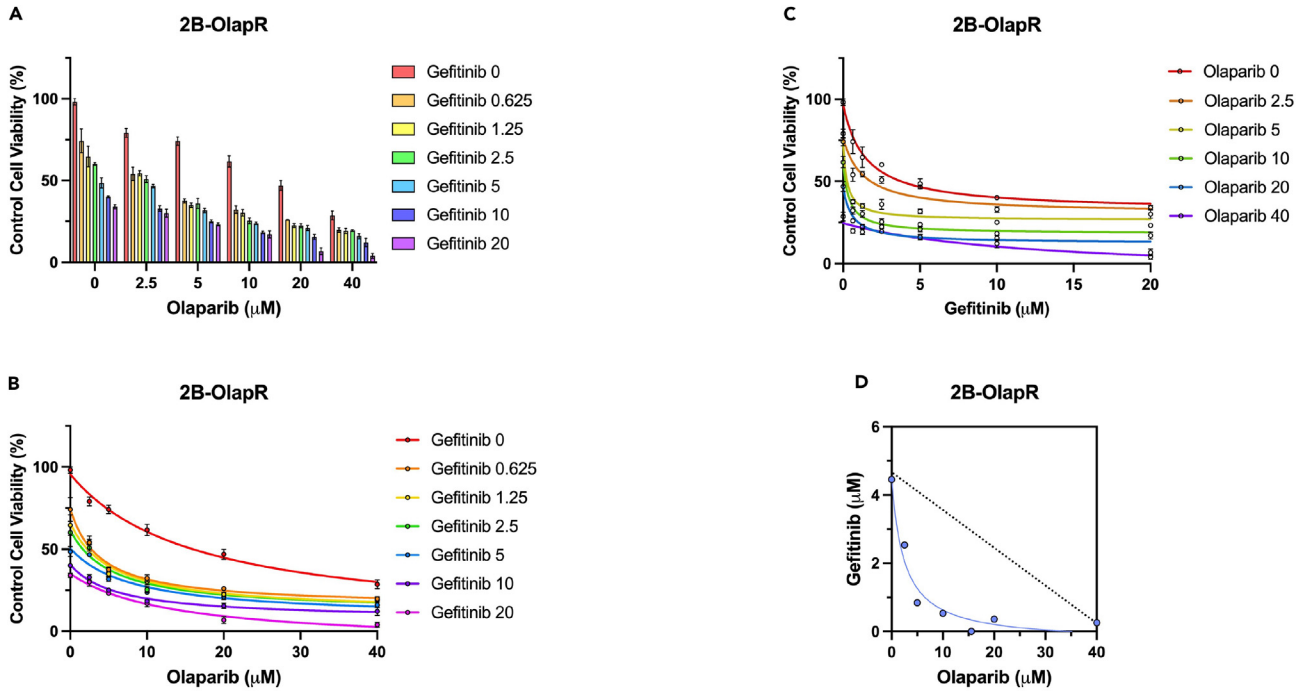

Figure 5. Gefitinib synergizes with Olaparib in the Olaparib-resistant CRPC, 2B-OlapR, cell line

(A) 2B-OlapR cells were treated with Olaparib (Ola) or Gefitinib (Gef) alone or combination at doses as indicated. The cell number was counted 2 days following the treatment and expressed as percentage to the control.

(B and C) Dose-response curves for the combination of Gefitinib and Olaparib. Data plotted as the concentration of Gefitinib vs. inhibition of cell viability, in the presence of increasing doses of Olaparib (B) and as the concentrations of Olaparib in the presence of increasing doses of Gefitinib (C).

(D) Isobologram analysis. The blue line represents the isobole derived from actual Olaparib-Gefitinib combinations that produce 50% inhibition. The diagonal, dotted line indicates additivity, and the data points below the line of additivity indicate synergy, data points above denote antagonism.

IGFBP3's overexpression appears to have a pronounced effect on DNA double-strand break (DSB) repair pathways. Whereas Olaparib induced DNA damage and subsequent apoptosis in LNCaP and C4-2B cells, this was not seen in the OlapR cells (Figure 1G). Intriguingly, IGFBP3 mRNA levels and γH2AX levels were seen to increase in conjunction in Olaparib-treated LNCaP and C4-2B cells, suggesting a potential link between IGFBP3 and DSB repair. This connection was further reinforced by the observation that OlapR models had significantly higher levels of γH2AX, suggesting that IGFBP3 overexpression enhances DSB repair, thereby promoting Olaparib resistance.

IGFBP3 has been identified as an activator of ligand-induced dimerization of EGFR.[65,66] Once dimerization occurs, EGFR becomes phosphorylated and translocates to the nucleus, where it triggers the autophosphorylation of DNAPKcs at the Ser2056 site, a critical step for the repair of double-strand breaks (DSBs) via non-homologous end-joining (NHEJ). We observed an increase in the phosphorylation levels of EGFR in both of our Olaparib-resistant OlapR cells. Concurrently, we detected an upregulation in the phosphorylation levels of DNAPKcs in OlapR cells. Furthermore, depletion of EGFR through siRNA resulted in a significant decrease in cell viability of 2B-OlapR cells and a substantial reduction in proliferation. These findings support the notion that the IGFBP3-EGFR interaction is crucial for promoting DNA repair mediated by DNAPKcs activation, thereby contributing to Olaparib resistance. Notably, EGFR is often highly expressed and activated in many cancers and is associated with poor prognosis. Specifically in the context of prostate cancer, EGFR overexpression has been linked to metastasis.[67] In patients with high Gleason score prostate cancer, upregulation of both EGFR and DNAPKcs has been identified (Figure 3D-F). Collectively, these data highlight the importance of the IGFBP3-EGFR-DNAPKcs signaling pathway in OlapR cells and suggest that targeting this pathway might present a novel therapeutic strategy for overcoming Olaparib resistance in prostate cancer.

With IGFBP3-EGFR-DNAPKcs identified as a key pathway to Olaparib resistance but currently lacking a small molecule inhibitor to IGFBP3, our attention was drawn to EGFR. Our studies had demonstrated the suppression of cell growth in 2B-OlapR cells through siRNA-mediated EGFR inhibition, leading us to further explore the use of pharmacological inhibitors to enhance Olaparib sensitivity. We found that treatment of OlapR models with the EGFR-targeting small molecule inhibitor, Gefitinib, resulted in significant growth inhibition of OlapR cells. Gefitinib suppressed the growth of OlapR cells in a dose-dependent manner, with IC_{50} values of 20.77μmol/L and 17.13μmol/L for LN-OlapR and 2B-OlapR cells, respectively. Considering the effect of IGFBP3 inhibition on re-sensitizing resistant models to Olaparib, we then investigated if similar results could be achieved with EGFR inhibition. Cell growth assays revealed that the combination of Olaparib and Gefitinib synergistically inhibited cell growth of OlapR cells, pointing to the possibility of using this drug combination to overcome Olaparib resistance. Further support for this strategy was provided by the Isobologram analysis, which demonstrated the synergistic cell growth inhibition by the

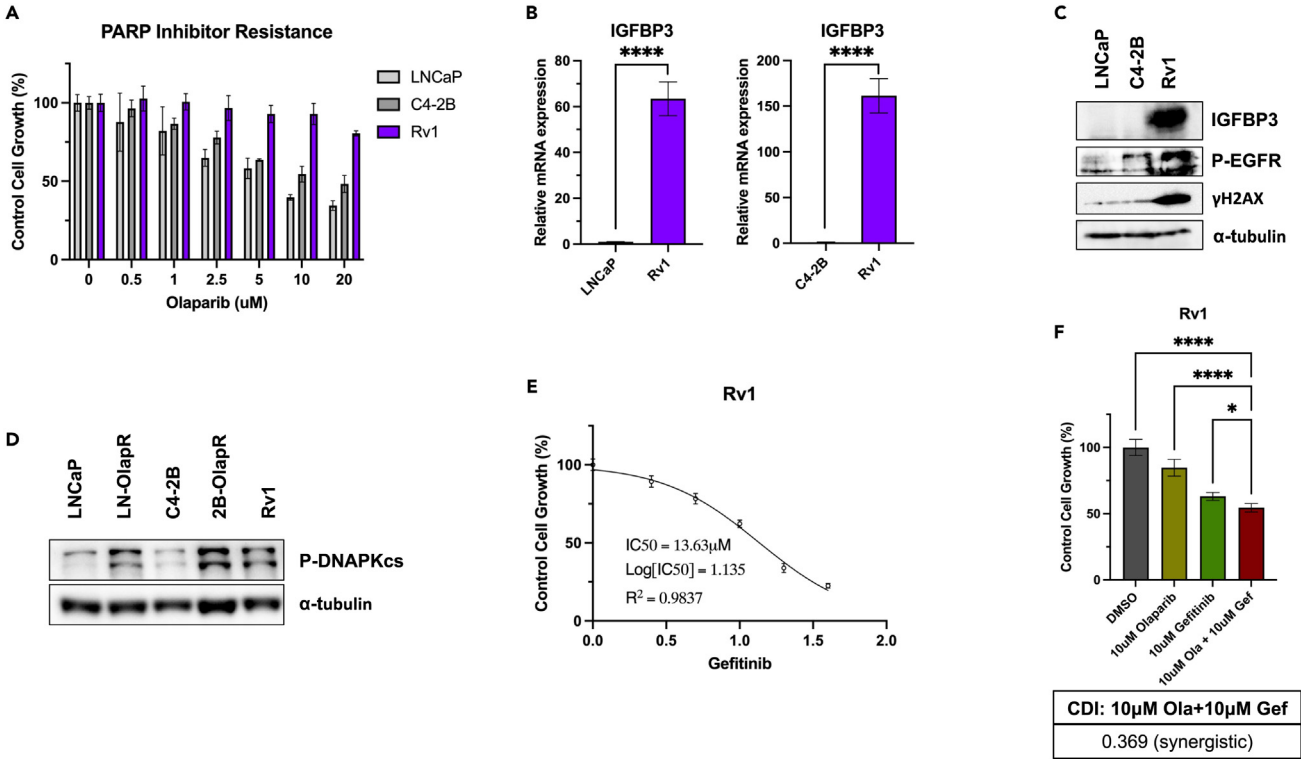

Figure 6. IGFBP3 and EGFR are overexpressed in the intrinsic Olaparib-resistant Rv1 cell line

(A) The cell growth of Rv1 cells versus LNCaP and C4-2B cells treated with increasing doses of Olaparib for 72 h demonstrate robust resistance to Olaparib was determined by CCK-8.

(B) Relative mRNA expression levels of IGFBP3 in Rv1 cells were determined by qPCR.

(C) The protein expression of IGFBP3, Phospho-EGF receptor (Tyr1068), and γH2AX in Rv1 cells was determined by western blot analysis. Tubulin served as a loading control.

(D) The protein expression of phospho-DNA-PKcs (Ser2056) in Rv1 cells was determined by western blot analysis. Tubulin served as a loading control.

(E) The IC50 value of Rv1 cells treated with Gefitinib via cell growth were determined by CCK-8.

(F) The cell growth of Rv1 treated with 10 μM Olaparib and 10 μM Gefitinib for 72 h was determined by CCK-8. The combination drug index (CDI) of Olaparib and Gefitinib in Rv1 was calculated. p value less than 0.05 was considered significant (*, $p < 0.05$; **, $p < 0.01$; ***, $p < 0.001$; ****, $p < 0.0001$). Statistical analysis was performed using Student's t test.

Olaparib-Gefitinib combination in 2B-OlapR cells. Finally, we examined the efficacy of this drug combination on 2B-OlapR cell-derived spheroids, which mimic the 3D architecture of tumors. Notably, the combination of Olaparib and Gefitinib significantly inhibited the viability of these spheroid cells. In conclusion, our results indicate that Gefitinib can alter Olaparib sensitivity, thereby phenocopying the effects of IGFBP3 inhibition, and presents a potential therapeutic strategy for overcoming Olaparib resistance in prostate cancer.

Our study on the OlapR models, specifically LN-OlapR and 2B-OlapR, offered insights into the mechanisms of acquired Olaparib resistance. To complement this understanding, we further evaluated the Rv1 cell line, a castration-resistant, AR-positive human prostate cancer model, to understand the intricacies of intrinsic Olaparib resistance. Rv1 cells demonstrated robust resistance toward Olaparib, underlining their utility as an intrinsic resistance model. Our data revealed a significant upregulation of IGFBP3 in Rv1 cells compared to LNCaP and C4-2B cells, echoing our earlier observations in OlapR models and supporting the potential involvement of IGFBP3 in intrinsic Olaparib resistance. The protein expression levels of P-EGFR, γH2AX, and IGFBP3 were elevated in Rv1 cells, as was the expression of P-DNAPKcs, reaffirming the role of the IGFBP3-EGFR-DNAPKcs pathway in PARPi resistance. Inhibition of IGFBP3 via siRNA knockdown resulted in a decrease in Rv1 cell proliferation and resensitized Rv1 cells to Olaparib treatment, concomitant with reduced IGFBP3 RNA and protein levels. Given the high levels of P-EGFR observed in Rv1 cells, we subsequently assessed the impact of EGFR inhibition via Gefitinib on Rv1 cell growth. We found that Gefitinib efficiently inhibited Rv1 cell growth, with an IC_{50} of 13.63μmol/L, and enhanced Olaparib activity. These findings further demonstrate that overexpression of IGFBP3 and EGFR serves as key mechanisms in both acquired and intrinsic Olaparib resistance.

In summary, we demonstrated that IGFBP3 is highly expressed in models of Olaparib resistance, both in acquired (LN-OlapR and 2B-OlapR cell lines) and intrinsic (Rv1 cells) resistance models. IGFBP3 inhibition led to decreased cell growth and increased Olaparib sensitivity, signifying its crucial role in maintaining Olaparib resistance. We also found that EGFR-DNAPKcs signaling, which is known to be potentiated by IGFBP3, was overexpressed in Olaparib resistant cells. Pharmacological inhibition of EGFR using Gefitinib resulted in decreased cell growth and improved Olaparib sensitivity, thereby phenocopying IGFBP3 inhibition. These findings highlight IGFBP3 and EGFR as critical

mediators of Olaparib resistance and suggest that targeting these molecules could be a promising strategy to overcome Olaparib resistance in advanced stages of prostate cancer.

Limitations of the study

We demonstrated that Olaparib plus IGFBP3 inhibition enhanced DNA damage and activated apoptosis; however, additional work is required to determine whether DNA damaged-induced cell death could result from combining IGFBP3 inhibition with other PARPi family members (Rucaparib, Talazoparib, or Niraparib). This study is limited to prostate cancer cells. The effect of IGFBP3 under various physiological conditions and cancer types will require further investigation. In addition, an effective and safe IGFBP3 inhibitor needs to be developed to translate these findings into clinics. We addressed most of our questions using *in vitro* experiments, but more physiological studies using animal models will be the next step in this line of research.

STAR★METHODS

Detailed methods are provided in the online version of this paper and include the following:

- KEY RESOURCES TABLE
- RESOURCE AVAILABILITY
  - Lead contact
  - Materials availability
  - Data and code availability
- EXPERIMENTAL MODEL AND STUDY PARTICIPANT DETAILS
  - Human cell lines and culture conditions
- METHOD DETAILS
  - Transcriptomics
  - Bioinformatics and data analysis
  - Cell growth assay
  - Drug synergy
  - Clonogenic assay
  - RNA isolation and RT-qPCR
  - Preparation of whole-cell lysates
  - Immunoblotting
  - Enzyme-linked immunosorbent assay
- QUANTIFICATION AND STATISTICAL ANALYSIS

SUPPLEMENTAL INFORMATION

Supplemental information can be found online at https://doi.org/10.1016/j.isci.2024.108984.

ACKNOWLEDGMENTS

This work was supported in part by grants CA253605 (A.C.G), CA 225836 (A.C.G), CA250082 (A.C.G), CA271327 (A.C.G), DOD PC180180 (A.C.G), NCI 1K01CA262351-01 (A.P.L), and the U.S. Department of Veterans Affairs, Office of Research & Development BL&D grant number I01BX004036 (A.C.G), BLR&D Research Career Scientist Award IK6BX005222 (A.C.G). A.C.G is also a Senior Research Career Scientist at VA Northern California Health Care System, Mather, California. The Genomics Shared Resource is supported by Cancer Center Support Grant P30CA093373 awarded by the NCI.

AUTHOR CONTRIBUTIONS

A.R.L., A.P.L., and A.C.G conceived and designed the study. A.R.L. was responsible for conducting the research, data analysis, and writing. A.R.L., A.P.L., S.N., and A.C.G. analyzed and interpreted the data. A.P.L., S.N., L.S.D., M.S., Z.A.S., and W.L. performed experiments. A.P.L., C.M.A., C.L., C.P.E., A.C.G. edited the writing. A.C.G. was responsible for experimental design, data analysis, writing, and supervision.

DECLARATION OF INTERESTS

The authors declare no competing interest.

Received: August 15, 2023
Revised: November 7, 2023
Accepted: January 17, 2024
Published: January 20, 2024

REFERENCES

1. Ferlay, J., Steliarova-Foucher, E., Lortet-Tieulent, J., Rosso, S., Coebergh, J.W.W., Comber, H., Forman, D., and Bray, F. (2013). Cancer incidence and mortality patterns in Europe: Estimates for 40 countries in 2012. Eur. J. Cancer *49*, 1374–1403. https://doi.org/10.1016/j.ejca.2012.12.027.
2. Heinlein, C.A., and Chang, C. (2004). Androgen receptor in prostate cancer. Endocr. Rev. *25*, 276–308. https://doi.org/10.1210/er.2002-0032.
3. Fujita, K., and Nonomura, N. (2019). Role of Androgen Receptor in Prostate Cancer: A Review. World J. Mens Health *37*, 288–295. https://doi.org/10.5534/wjmh.180040.
4. Harris, W.P., Mostaghel, E.A., Nelson, P.S., and Montgomery, B. (2009). Androgen deprivation therapy: progress in understanding mechanisms of resistance and optimizing androgen depletion. Nature clinical practice. Urology *6*, 76–85. https://doi.org/10.1038/ncpuro1296.
5. Shafi, A.A., Cox, M.B., and Weigel, N.L. (2013). Androgen receptor splice variants are resistant to inhibitors of Hsp90 and FKBP52, which alter androgen receptor activity and expression. Steroids *78*, 548–554. https://doi.org/10.1016/j.steroids.2012.12.013.
6. Huggins, C., and Hodges, C.V. (1972). Studies on prostatic cancer. I. The effect of castration, of estrogen and androgen injection on serum phosphatases in metastatic carcinoma of the prostate. CA Cancer J. Clin. *22*, 232–240.
7. Feng, Q., and He, B. (2019). Androgen Receptor Signaling in the Development of Castration-Resistant Prostate Cancer. Front. Oncol. *9*, 858. https://doi.org/10.3389/fonc.2019.00858.
8. Armstrong, C.M., and Gao, A.C. (2015). Drug resistance in castration resistant prostate cancer: resistance mechanisms and emerging treatment strategies. Am. J. Clin. Exp. Urol. *3*, 64–76.
9. Sternberg, C.N., Petrylak, D.P., Madan, R.A., and Parker, C. (2014). Progress in the treatment of advanced prostate cancer. Am. Soc. Clin. Oncol. Educ. Book, 117–131. https://doi.org/10.14694/EdBook_AM.2014.34.117.
10. Tran, C., Ouk, S., Clegg, N.J., Chen, Y., Watson, P.A., Arora, V., Wongvipat, J., Smith-Jones, P.M., Yoo, D., Kwon, A., et al. (2009). Development of a second-generation antiandrogen for treatment of advanced prostate cancer. Science *324*, 787–790. https://doi.org/10.1126/science.1168175.
11. Nadiminty, N., Tummala, R., Liu, C., Yang, J., Lou, W., Evans, C.P., and Gao, A.C. (2013). NF-κB2/p52 induces resistance to enzalutamide in prostate cancer: role of androgen receptor and its variants. Mol. Cancer Therapeut. *12*, 1629–1637. https://doi.org/10.1158/1535-7163.MCT-13-0027.
12. Joseph, J.D., Lu, N., Qian, J., Sensintaffar, J., Shao, G., Brigham, D., Moon, M., Maneval, E.C., Chen, I., Darimont, B., and Hager, J.H. (2013). A clinically relevant androgen receptor mutation confers resistance to second-generation antiandrogens enzalutamide and ARN-509. Cancer Discov. *3*, 1020–1029. https://doi.org/10.1158/2159-8290.CD-13-0226.
13. Antonarakis, E.S., Lu, C., Wang, H., Luber, B., Nakazawa, M., Roeser, J.C., Chen, Y., Mohammad, T.A., Chen, Y., Fedor, H.L., et al. (2014). AR-V7 and resistance to enzalutamide and abiraterone in prostate cancer. N. Engl. J. Med. *371*, 1028–1038. https://doi.org/10.1056/NEJMoa1315815.
14. Chen, A. (2011). PARP inhibitors: its role in treatment of cancer. Chin. J. Cancer *30*, 463–471. https://doi.org/10.5732/cjc.011.10111.
15. Tisseverasinghe, S., Bahoric, B., Anidjar, M., Probst, S., and Niazi, T. (2023). Advances in PARP Inhibitors for Prostate Cancer. Cancers *15*, 1849. https://doi.org/10.3390/cancers15061849.
16. Helleday, T. (2011). The underlying mechanism for the PARP and BRCA synthetic lethality: clearing up the misunderstandings. Mol. Oncol. *5*, 387–393. https://doi.org/10.1016/j.molonc.2011.07.001.
17. Ghose, A., Moschetta, M., Pappas-Gogos, G., Sheriff, M., and Boussios, S. (2021). Genetic Aberrations of DNA Repair Pathways in Prostate Cancer: Translation to the Clinic. Int. J. Mol. Sci. *22*, 9783. https://doi.org/10.3390/ijms22189783.
18. Cousineau, I., Abaji, C., and Belmaaza, A. (2005). BRCA1 regulates RAD51 function in response to DNA damage and suppresses spontaneous sister chromatid replication slippage: implications for sister chromatid cohesion, genome stability, and carcinogenesis. Cancer Res. *65*, 11384–11391. https://doi.org/10.1158/0008-5472.CAN-05-2156.
19. Abaji, C., Cousineau, I., and Belmaaza, A. (2005). BRCA2 regulates homologous recombination in response to DNA damage: implications for genome stability and carcinogenesis. Cancer Res. *65*, 4117–4125. https://doi.org/10.1158/0008-5472.CAN-04-3071.
20. Zong, C., Zhu, T., He, J., Huang, R., Jia, R., and Shen, J. (2022). PARP mediated DNA damage response, genomic stability and immune responses. Int. J. Cancer *150*, 1745–1759. https://doi.org/10.1002/ijc.33918.
21. Obaji, E., Maksimainen, M.M., Galera-Prat, A., and Lehtiö, L. (2021). Activation of PARP2/ARTD2 by DNA damage induces conformational changes relieving enzyme autoinhibition. Nat. Commun. *12*, 3479. https://doi.org/10.1038/s41467-021-23800-x.
22. de Bono, J., Mateo, J., Fizazi, K., Saad, F., Shore, N., Sandhu, S., Chi, K.N., Sartor, O., Agarwal, N., Olmos, D., et al. (2020). Olaparib for Metastatic Castration-Resistant Prostate Cancer. N. Engl. J. Med. *382*, 2091–2102. https://doi.org/10.1056/NEJMoa1911440.
23. Mateo, J., Carreira, S., Sandhu, S., Miranda, S., Mossop, H., Perez-Lopez, R., Nava Rodrigues, D., Robinson, D., Omlin, A., Tunariu, N., et al. (2015). DNA-Repair Defects and Olaparib in Metastatic Prostate Cancer. N. Engl. J. Med. *373*, 1697–1708. https://doi.org/10.1056/NEJMoa1506859.
24. Criscuolo, D., Morra, F., Giannella, R., Cerrato, A., and Celetti, A. (2019). Identification of Novel Biomarkers of Homologous Recombination Defect in DNA Repair to Predict Sensitivity of Prostate Cancer Cells to PARP-Inhibitors. Int. J. Mol. Sci. *20*, 3100. https://doi.org/10.3390/ijms20123100.
25. Gorodetska, I., Kozeretska, I., and Dubrovska, A. (2019). Genes: The Role in Genome Stability, Cancer Stemness and Therapy Resistance. J. Cancer *10*, 2109–2127. https://doi.org/10.7150/jca.30410.
26. Boussios, S., Rassy, E., Shah, S., Ioannidou, E., Sheriff, M., and Pavlidis, N. (2021). Aberrations of DNA repair pathways in prostate cancer: a cornerstone of precision oncology. Expert Opin. Ther. Targets *25*, 329–333. https://doi.org/10.1080/14728222.2021.1951226.
27. Caffo, O., Veccia, A., Kinspergher, S., Rizzo, M., and Maines, F. (2018). Aberrations of DNA Repair Pathways in Prostate Cancer: Future Implications for Clinical Practice? Front. Cell Dev. Biol. *6*, 71. https://doi.org/10.3389/fcell.2018.00071.
28. Pritchard, C.C., Mateo, J., Walsh, M.F., De Sarkar, N., Abida, W., Beltran, H., Garofalo, A., Gulati, R., Carreira, S., Eeles, R., et al. (2016). Inherited DNA-Repair Gene Mutations in Men with Metastatic Prostate Cancer. N. Engl. J. Med. *375*, 443–453. https://doi.org/10.1056/NEJMoa1603144.
29. Beltran, H., Yelensky, R., Frampton, G.M., Park, K., Downing, S.R., MacDonald, T.Y., Jarosz, M., Lipson, D., Tagawa, S.T., Nanus, D.M., et al. (2013). Targeted next-generation sequencing of advanced prostate cancer identifies potential therapeutic targets and disease heterogeneity. Eur. Urol. *63*, 920–926. https://doi.org/10.1016/j.eururo.2012.08.053.
30. Robinson, D., Van Allen, E.M., Wu, Y.M., Schultz, N., Lonigro, R.J., Mosquera, J.M., Montgomery, B., Taplin, M.E., Pritchard, C.C., Attard, G., et al. (2015). Integrative Clinical Genomics of Advanced Prostate Cancer. Cell *162*, 454. https://doi.org/10.1016/j.cell.2015.06.053.
31. Asim, M., Tarish, F., Zecchini, H.I., Sanjiv, K., Gelali, E., Massie, C.E., Baridi, A., Warren, A.Y., Zhao, W., Ogris, C., et al. (2017). Synthetic lethality between androgen receptor signalling and the PARP pathway in prostate cancer. Nat. Commun. *8*, 374. https://doi.org/10.1038/s41467-017-00393-y.
32. Lee, E.K., and Matulonis, U.A. (2020). PARP Inhibitor Resistance Mechanisms and Implications for Post-Progression Combination Therapies. Cancers *12*, 2054. https://doi.org/10.3390/cancers12082054.
33. Livraghi, L., and Garber, J.E. (2015). PARP inhibitors in the management of breast cancer: current data and future prospects. BMC Med. *13*, 188. https://doi.org/10.1186/s12916-015-0425-1.
34. von Werdt, A., Brandt, L., Schärer, O.D., and Rubin, M.A. (2021). PARP Inhibition in Prostate Cancer With Homologous Recombination Repair Alterations. JCO Precis. Oncol. *5*, 1639–1649. https://doi.org/10.1200/PO.21.00152.
35. Pettitt, S.J., Frankum, J.R., Punta, M., Lise, S., Alexander, J., Chen, Y., Yap, T.A., Haider, S., Tutt, A.N.J., and Lord, C.J. (2020). Clinical BRCA1/2 Reversion Analysis Identifies Hotspot Mutations and Predicted Neoantigens Associated with Therapy Resistance. Cancer Discov. *10*, 1475–1488. https://doi.org/10.1158/2159-8290.CD-19-1485.
36. Darabi, S., Braxton, D.R., Xiu, J., Carneiro, B.A., Swensen, J., Antonarakis, E.S., Liu, S.V., McKay, R.R., Spetzler, D., El-Deiry, W.S., and Demeure, M.J. (2022). Reversion Mutations in Patients Treated with Poly ADP-Ribose Polymerase (PARP) Inhibitors or Platinum Agents. Medicina *58*, 1818. https://doi.org/10.3390/medicina58121818.
37. Lombard, A.P., Armstrong, C.M., D'Abronzo, L.S., Ning, S., Leslie, A.R., Sharifi, M., Lou, W., Evans, C.P., Dall'Era, M., Chen, H.W., et al. (2022). Olaparib-Induced Senescence Is

Bypassed through G2-M Checkpoint Override in Olaparib-Resistant Prostate Cancer. Mol. Cancer Therapeut. *21*, 677–685. https://doi.org/10.1158/1535-7163.MCT-21-0604.

38. Podhorecka, M., Skladanowski, A., and Bozko, P. (2010). H2AX Phosphorylation: Its Role in DNA Damage Response and Cancer Therapy. J. Nucleic Acids *2010*, 920161. https://doi.org/10.4061/2010/920161.
39. Collins, P.L., Purman, C., Porter, S.I., Nganga, V., Saini, A., Hayer, K.E., Gurewitz, G.L., Sleckman, B.P., Bednarski, J.J., Bassing, C.H., and Oltz, E.M. (2020). DNA double-strand breaks induce H2Ax phosphorylation domains in a contact-dependent manner. Nat. Commun. *11*, 3158. https://doi.org/10.1038/s41467-020-16926-x.
40. Mao, Z., Bozzella, M., Seluanov, A., and Gorbunova, V. (2008). Comparison of nonhomologous end joining and homologous recombination in human cells. DNA Repair *7*, 1765–1771. https://doi.org/10.1016/j.dnarep.2008.06.018.
41. Brandsma, I., and Gent, D.C. (2012). Pathway choice in DNA double strand break repair: observations of a balancing act. Genome Integr. *3*, 9. https://doi.org/10.1186/2041-9414-3-9.
42. Hensley, P.J., Cao, Z., Pu, H., Dicken, H., He, D., Zhou, Z., Wang, C., Koochekpour, S., and Kyprianou, N. (2019). Predictive and targeting value of IGFBP-3 in therapeutically resistant prostate cancer. Am. J. Clin. Exp. Urol. *7*, 188–202.
43. Baxter, R.C. (2013). Insulin-like growth factor binding protein-3 (IGFBP-3): Novel ligands mediate unexpected functions. J. Cell Commun. Signal. *7*, 179–189. https://doi.org/10.1007/s12079-013-0203-9.
44. Hammel, M., Yu, Y., Mahaney, B.L., Cai, B., Ye, R., Phipps, B.M., Rambo, R.P., Hura, G.L., Pelikan, M., So, S., et al. (2010). Ku and DNA-dependent protein kinase dynamic conformations and assembly regulate DNA binding and the initial non-homologous end joining complex. J. Biol. Chem. *285*, 1414–1423. https://doi.org/10.1074/jbc.M109.065615.
45. Lin, M.Z., Marzec, K.A., Martin, J.L., and Baxter, R.C. (2014). The role of insulin-like growth factor binding protein-3 in the breast cancer cell response to DNA-damaging agents. Oncogene *33*, 85–96. https://doi.org/10.1038/onc.2012.538.
46. Martin, J.L., Lin, M.Z., McGowan, E.M., and Baxter, R.C. (2009). Potentiation of growth factor signaling by insulin-like growth factor-binding protein-3 in breast epithelial cells requires sphingosine kinase activity. J. Biol. Chem. *284*, 25542–25552. https://doi.org/10.1074/jbc.M109.007120.
47. Sakata, J., Hirosue, A., Yoshida, R., Matsuoka, Y., Kawahara, K., Arita, H., Nakashima, H., Yamamoto, T., Nagata, M., Kawaguchi, S., et al. (2020). Enhanced Expression of IGFBP-3 Reduces Radiosensitivity and Is Associated with Poor Prognosis in Oral Squamous Cell Carcinoma. Cancers *12*, 494. https://doi.org/10.3390/cancers12020494.
48. Namekawa, T., Ikeda, K., Horie-Inoue, K., and Inoue, S. (2019). Application of Prostate Cancer Models for Preclinical Study: Advantages and Limitations of Cell Lines, Patient-Derived Xenografts, and Three-Dimensional Culture of Patient-Derived Cells. Cells *8*. https://doi.org/10.3390/cells8010074.
49. Feiersinger, G.E., Trattnig, K., Leitner, P.D., Guggenberger, F., Oberhuber, A., Peer, S., Hermann, M., Skvortsova, I., Vrbkova, J., Bouchal, J., et al. (2018). Olaparib is effective in combination with, and as maintenance therapy after, first-line endocrine therapy in prostate cancer cells. Mol. Oncol. *12*, 561–576. https://doi.org/10.1002/1878-0261.12185.
50. Zhang, D., Xu, X., Wei, Y., Chen, X., Li, G., Lu, Z., Zhang, X., Ren, X., Wang, S., and Qin, C. (2022). Prognostic Role of DNA Damage Response Genes Mutations and their Association With the Sensitivity of Olaparib in Prostate Cancer Patients. Cancer Control *29*. https://doi.org/10.1177/10732748221129451.
51. Brenner, J.C., Ateeq, B., Li, Y., Yocum, A.K., Cao, Q., Asangani, I.A., Patel, S., Wang, X., Liang, H., Yu, J., et al. (2011). Mechanistic rationale for inhibition of poly(ADP-ribose) polymerase in ETS gene fusion-positive prostate cancer. Cancer Cell *19*, 664–678. https://doi.org/10.1016/j.ccr.2011.04.010.
52. Chan, J.M., Stampfer, M.J., Ma, J., Gann, P., Gaziano, J.M., Pollak, M., and Giovannucci, E. (2002). Insulin-like growth factor-I (IGF-I) and IGF binding protein-3 as predictors of advanced-stage prostate cancer. J. Natl. Cancer Inst. *94*, 1099–1106. https://doi.org/10.1093/jnci/94.14.1099.
53. Bao, L., Liu, H., You, B., Gu, M., Shi, S., Shan, Y., Li, L., Chen, J., and You, Y. (2016). Overexpression of IGFBP3 is associated with poor prognosis and tumor metastasis in nasopharyngeal carcinoma. Tumour Biol. *37*, 15043–15052. https://doi.org/10.1007/s13277-016-5400-8.
54. Seligson, D.B., Yu, H., Tze, S., Said, J., Pantuck, A.J., Cohen, P., and Lee, K.W. (2013). IGFBP-3 nuclear localization predicts human prostate cancer recurrence. Horm. Cancer *4*, 12–23. https://doi.org/10.1007/s12672-012-0124-8.
55. Liao, H., Ji, F., Helleday, T., and Ying, S. (2018). Mechanisms for stalled replication fork stabilization: new targets for synthetic lethality strategies in cancer treatments. EMBO Rep. *19*, e46263. https://doi.org/10.15252/embr.201846263.
56. Meyn, R.E., Munshi, A., Haymach, J.V., Milas, L., and Ang, K.K. (2009). Receptor signaling as a regulatory mechanism of DNA repair. Radiother. Oncol. *92*, 316–322. https://doi.org/10.1016/j.radonc.2009.06.031.
57. Volman, Y., Hefetz, R., Galun, E., and Rachmilewitz, J. (2022). DNA damage alters EGFR signaling and reprograms cellular response via Mre-11. Sci. Rep. *12*, 5760. https://doi.org/10.1038/s41598-022-09779-5.
58. Masuda, H., Zhang, D., Bartholomeusz, C., Doihara, H., Hortobagyi, G.N., and Ueno, N.T. (2012). Role of epidermal growth factor receptor in breast cancer. Breast Cancer Res. Treat. *136*, 331–345. https://doi.org/10.1007/s10549-012-2289-9.
59. Nastały, P., Stoupiec, S., Popęda, M., Śmentoch, J., Schlomm, T., Morrissey, C., Żaczek, A.J., Beyer, B., Tennstedt, P., Graefen, M., et al. (2020). EGFR as a stable marker of prostate cancer dissemination to bones. Br. J. Cancer *123*, 1767–1774. https://doi.org/10.1038/s41416-020-01052-8.
60. Zhao, Y., Gao, J.L., Ji, J.W., Gao, M., Yin, Q.S., Qiu, Q.L., Wang, C., Chen, S.Z., Xu, J., Liang, R.S., et al. (2014). Cytotoxicity enhancement in MDA-MB-231 cells by the combination treatment of tetrahydropalmatine and berberine derived from Corydalis yanhusuo W. T. Wang. J. Intercult. Ethnopharmacol. *3*, 68–72. https://doi.org/10.5455/jice.20140123040224.
61. Huang, R.Y., Pei, L., Liu, Q., Chen, S., Dou, H., Shu, G., Yuan, Z.X., Lin, J., Peng, G., Zhang, W., and Fu, H. (2019). Isobologram Analysis: A Comprehensive Review of Methodology and Current Research. Front. Pharmacol. *10*, 1222. https://doi.org/10.3389/fphar.2019.01222.
62. Wang, X., Zhang, H., and Chen, X. (2019). Drug resistance and combating drug resistance in cancer. Cancer Drug Resist. *2*, 141–160. https://doi.org/10.20517/cdr.2019.10.
63. Han, W., Gao, S., Barrett, D., Ahmed, M., Han, D., Macoska, J.A., He, H.H., and Cai, C. (2018). Reactivation of androgen receptor-regulated lipid biosynthesis drives the progression of castration-resistant prostate cancer. Oncogene *37*, 710–721. https://doi.org/10.1038/onc.2017.385.
64. Cancer Genome Atlas Research Network (2015). The Molecular Taxonomy of Primary Prostate Cancer. Cell *163*, 1011–1025. https://doi.org/10.1016/j.cell.2015.10.025.
65. Martin, J.L., Weenink, S.M., and Baxter, R.C. (2003). Insulin-like growth factor-binding protein-3 potentiates epidermal growth factor action in MCF-10A mammary epithelial cells. Involvement of p44/42 and p38 mitogen-activated protein kinases. J. Biol. Chem. *278*, 2969–2976. https://doi.org/10.1074/jbc.M210739200.
66. Varma Shrivastav, S., Bhardwaj, A., Pathak, K.A., and Shrivastav, A. (2020). Insulin-Like Growth Factor Binding Protein-3 (IGFBP-3): Unraveling the Role in Mediating IGF-Independent Effects Within the Cell. Front. Cell Dev. Biol. *8*, 286. https://doi.org/10.3389/fcell.2020.00286.
67. Chen, T., Xu, J., and Fu, W. (2020). EGFR/FOXO3A/LXR-α Axis Promotes Prostate Cancer Proliferation and Metastasis and Dual-Targeting LXR-α/EGFR Shows Synthetic Lethality. Front. Oncol. *10*, 1688. https://doi.org/10.3389/fonc.2020.01688.

STAR★METHODS

KEY RESOURCES TABLE

REAGENT or RESOURCE	SOURCE	IDENTIFIER
Antibodies		
IGFBP3	Santa Cruz Biotechnology	Cat# SC-365936, RRID: AB_10917037
Phospho-Histone H2A.X (Ser139)	Cell Signaling Technology	Cat#: 9718, RRID: AB_2118009
Cleaved PARP	Cell Signaling Technology	Cat#: 9541, RRID: AB_331426
Phospho-DNA-PKcs (Ser2056)	Cell Signaling Technology	Cat#: 68716, RRID: AB_2939025
Phospho-EGF Receptor (Tyr1068)	Cell Signaling Technology	Cat#: 2234, RRID: AB_331701
EGF Receptor	Cell Signaling Technology	Cat#: 4267, RRID: AB_2246311
DNA-PKcs	Cell Signaling Technology	Cat#: 4602, RRID: AB_10692482
Alpha Tubulin	Santa Cruz Biotechnology	Cat#: sc-5286, AB_628411
Anti-Rabbit	ThermoFisher Scientific	Cat#: NC0161557, RRID: AB_218567
Anti-Mouse	ThermoFisher Scientific	Cat#: NC9575145, RRID: AB_218457
Chemicals, peptides, and recombinant proteins		
Olaparib (AZD2281)	Selleck Chemicals	Cat#: S1060, CAS: 763113-22-0
Gefitinib	MedChemExpress	Cat#: HY-50895, CAS: 184475-35-2
DMSO	Corning	Cat#: 25-950-CQC
Negative Control DsiRNA	Integrated DNA Technologies	Cat#: 51-01-14-04
Lipofectamine RNAiMAX Transfection Reagent	ThermoFisher Scientific	Cat#: 13778150
Opti-MEM	Gibco	Cat#: 31985088
TRIzol	ThermoFisher Scientific	Cat#: 15596018
RNase-free DNase	ThermoFisher Scientific	Cat#: FEREN0521
ImProm-II Reverse Transcriptase	Promega	Cat#: PR-A3802
SsoFast EvaGreen Supermix	BioRad	Cat#: 1725205
Halt Protease Inhibitor Cocktail (100X)	ThermoFisher Scientific	Cat#: 78430
Immobilon Crescendo Western HRP substrate	Millipore	Cat#: WBLUR0500
Recombinant Human IGFBP-3	R&D systems	Cat#: 675-B3
Recombinant Human Epidermal Growth Factor (EGF)	Gibco	Cat#: PHG0313
Crystal Violet	ThermoFisher Scientific	Cat#: C581-25
BIOFLOAT 96-well ultra-low attachment plate	faCellitate	Cat#: F202003
RPMI 1640	Corning	Cat#: MT10040CV
Fetal Bovine Serum (FBS)	Corning	Cat#: 35-010-CV
Penicillin-Streptomycin Solution (100x)	Corning	Cat#: 30-002-CI
Dulbecco's Phosphate-Buffered Saline (DPBS) (1x)	Corning	Cat#: 21-031-CV
0.5% Trypsin-EDTA (10x)	Gibco	Cat#: 15-400-054
Critical commercial assays		
Mycoplasma PCR Detection Kit	Applied Biological Materials	Cat#: G238
Pierce Bradford Plus Protein Assay Kits	ThermoFisher Scientific	Cat#: 23236
Cell Counting Kit-8 (CCK-8)	Dojindo Molecular Technologies	Cat#: CK04
Cell Titer-Glo 2.0 Cell Viability Assay	Promega	Cat#: G9242
NEB Next Ultra Directional RNA Library Prep Kit	New England BioLabs	Cat#: E7420
Human IGFBP-3 ELISA Kit	Sigma-Aldrich	Cat#: RAB0235
Human EGFR [pY1068] ELISA Kit	Invitrogen	Cat#: KHR9081

(*Continued on next page*)

Continued

REAGENT or RESOURCE	SOURCE	IDENTIFIER
Deposited data		
RNAseq Data	This paper	GSE249514
Prostate Cancer (DKFZ, Cancer Cell 2018)	cBioPortal	http://www.cbioportal.org
Prostate Adenocarcinoma (TCGA, Cell 2015)	cBioPortal	http://www.cbioportal.org
Metastatic Prostate Adenocarcinoma (SU2C/PCF Dream Team, PNAS 2019)	cBioPortal	http://www.cbioportal.org
Prostate Adenocarcinoma (Broad/Cornell, Nat Genet 2012)	cBioPortal	http://www.cbioportal.org
Experimental models: Cell lines		
LNCaP	ATCC	CRL-1740
C4-2B	ATCC	CRL-3315
22Rv1	ATCC	CRL-2505
LN-OlapR	Lombard et al.	N/A
2B-OlapR	Lombard et al.	N/A
Oligonucleotides		
IGFBP3 DsiRNA	Integrated DNA Technologies	Cat#: hs.Ri.IGFBP3.13.1 Sequence: 5′-rArArUrGrGrUrArArAr CrUrUrGrArGrCrArUrCrUrUrUrUCA-3′
EGFR DsiRNA	Integrated DNA Technologies	Cat#: hs.Ri.EGFR.13.3 Sequence 5′-rCrGrGrArArUrArGrGrUrArUrUrGr GrUrGrArArUrUrUrAAA-3′
IGFBP3 qPCR Primer	Integrated DNA Technologies	5′- ATGCAGCGGGCGCGAC 3′- CTACTTGCTCTGCATGCTGTAGCA
Actin qPCR Primer	Integrated DNA Technologies	5′-CCCAGCCATGTACGTTGCTA 3′-AGGGCATACC- CCTCGTAGATG
Software and algorithms		
cBioPortal	cBioPortal	http://www.cbioportal.org
GraphPad Prism 10.0	GraphPad	https://www.graphpad.com/
Gene Set Enrichment Analysis (GSEA) 4.1.0	UC San Diego and Broad Institute	https://www.gsea-msigdb.org/gsea/index.jsp
ImageJ	National Institutes of Health (NIH)	https://imagej.nih.gov/

RESOURCE AVAILABILITY

Lead contact

Further information and requests for resources and reagents should be directed to and will be fulfilled by the lead contact, Dr. Allen Gao (acgao@ucdavis.edu).

Materials availability

This study did not generate any unique reagents.

Data and code availability

- RNA-seq data have been deposited at GEO and are publicly available as of the date of publication. This paper analyzes existing, publicly available data. Accession numbers are listed in the key resources table. All the data reported in this study will be shared by the lead contact upon request.
- This study does not report any original code.
- Any additional information required to reanalyze the data reported in this paper is available from the lead contact upon request.

EXPERIMENTAL MODEL AND STUDY PARTICIPANT DETAILS

Human cell lines and culture conditions

Human PC cell lines LNCaP, C4-2B, and 22Rv1 were obtained from American Type Culture Collection (ATCC, Manassas, VA, USA). All cell lines were derived from male donors. ATCC uses short tandem repeat profiling for testing and authentication of cell lines. LNCaP, C4-2B, and Rv1 cells were maintained in RPMI 1640 (Corning, NY, USA) supplemented with 10% fetal bovine serum (FBS) (Corning, NY, USA), 100 IU penicillin (Corning, NY, USA), and 0.1 mg/mL streptomycin. Olaparib-resistant LN-OlapR and 2B-OlapR cells were derived from LNCaP and C4-2B cells respectively through chronic exposure to increasing doses of Olaparib (Selleck Chemicals, Houston, TX, USA) for over 1 year as described previously.[37] Both OlapR cell lines are maintained in complete RPMI 1640 supplemented with 5 mmol/L Olaparib. LNCaP and C4-2B cells were cultured alongside OlapR derivative cell lines as appropriate controls. All cell lines are routinely tested for mycoplasma using Mycoplasma PCR Detection Kit purchased from Applied Biological Materials (Richmond, CA). All experiments with these cell lines and their derivatives were conducted within 6 months of receipt or resuscitation after cryopreservation. Cell cultures were maintained at 37°C in a humidified incubator with 5% carbon dioxide. Olaparib (Cat#: S1060, CAS: 763113-22-0) was purchased from Selleck Chemicals (Houston, TX, USA). Gefitinib (Cat#: HY-50895, CAS: 184475-35-2) was purchased from MedChemExpress (Monmouth Junction, NJ, USA).

METHOD DETAILS

Transcriptomics

RNA samples were submitted to the UC Davis Comprehensive Cancer Center's Genomics Shared Resource (GSR) for RNA-sequencing (RNA-seq) analysis. Stranded mRNA-Sequencing libraries were prepared from 100 ng total RNA using Next Ultra Directional RNA Library Prep Kit (Cat#: E7420) purchased from New England BioLabs (Ipswich, MA, USA) according to the manufacturer's standard protocol, and as previously described. Subsequently, libraries were combined for multiplex sequencing on an Illumina HiSeq 4000 System (2 × 150 bp, paired-end, ≥20 × 106 reads per sample). Demultiplexed raw sequence data (FASTQ) were analyzed with a HISAT-StringTie-Cufflinks pipeline for read mapping to the human reference genome assembly (Dec. 2013, GRCh38/hg38), followed by transcript assembly and quantification of expression values as read counts. Principal component analysis (PCA) was conducted on the read counts gene-level data for all genes/transcripts passing filter (Filtered on Expression > 0.1) in the raw data (GEO accession number: GSE249514).

Bioinformatics and data analysis

Clinical datasets were analyzed using the cBioPortal for Cancer Genomics (http://www.cbioportal.org/).[64] The levels of IGFBP3, EGFR, and PRKDC mRNA in both normal prostate and PCa tissues were evaluated by analyzing multiple PCa mRNA datasets obtained from cBioPortal database. Further analysis was performed by dividing the patients into two groups based on Gleason Scores levels.

Cell growth assay

Cells were seeded at a density of 25,000 cells per well in twenty-four well plates in complete RPMI-1640 (Corning, NY, USA) media without any selection agent. After 24 h, cells were subjected to indicated treatments. RNAi was performed using Dicer-Substrate siRNAs (DsiRNA) purchased from Integrated DNA Technologies (Coralville, IA, USA) and Opti-MEM (Cat#: 31985088) from Gibco (Billings, MT, USA). The following DsiRNAs were used: Negative Control (NC) (Cat#: 51-01-14-04), IGFBP3 (Cat#: hs.Ri.IGFBP3.13.1), and EGFR (Cat#: hs.Ri.EGFR.13.1). Transfection of DsiRNAs was done using Lipofectamine RNAiMAX Transfection Reagent (Cat#: 13778150) purchased from ThermoFisher Scientific (Milton Park, UK) according to the manufacturer's protocol with 25 or 50 nmol/L DsiRNA. For experiments combining RNAi with drug, transfection of DsiRNA was performed 24 h after plating and drug was administered as indicated the following day. To determine synergism, the coefficient of drug interaction (CDI) and combination index (CI) is calculated as follows: CDI = AB/(A × B).[60] The CDIs were analyzed to determine the synergism of the two drugs in combination (A CDI value < 1, = 1, or >1 indicates that the drugs are synergistic, additive, or antagonistic respectively). Cell count was determined using Cell Counting Kit-8 (Cat#: CK04) purchased from Dojindo Molecular Technologies (Rockville, MD, USA). Data are displayed as percentage of control cell growth. Alternatively, total cells were counted via Beckman Coulter Particle Counter (Brea, CA, USA) 72 h after treatment. Microscopy was performed using a Keyence BZ-X810 imaging system. All conditions were performed either in triplicate or quadruplicate.

Drug synergy

Cells were plated at a density of 2000 cells per well in ninety-six well plates in complete RPMI-1640 (Corning, NY, USA) media without any selection agent. After 24 h, cells were subjected to indicated treatments. To further define drug synergy and evaluate drug interactions, an Isobologram is a graph of lines of constant effect that measures the drug effect of each dosage point using isoboles, which are lines joining the points of equal measured effect.[61] Cell viability was determined using Cell Titer-Glo 2.0 Cell Viability Assay (Cat#: G9242) from Promega (Madison, WI, USA). All conditions were performed either in triplicate.

Clonogenic assay

For the colony formation assay, cells were seeded at a density of 1000 cells per well in six-well plates. Subsequently, cells were treated as indicated and allowed to grow for 14 days. The colonies were rinsed with PBS before being fixed and stained with 4% paraformaldehyde

and 0.1% crystal violet (Cat#: C581-25) for 30 min. The colonies were quantified using ImageJ software (National Institutes of Health). All conditions were performed in triplicate.

RNA isolation and RT-qPCR

Total RNA was harvested using TRIzol reagent (Cat#: 15596018) purchased from ThermoFisher Scientific (Milton Park, UK) and RNA was digested with RNase-free DNase 1 (Cat#: FEREN0521) purchased from ThermoFisher Scientific (Milton Park, UK). The cDNA was prepared using ImProm-II reverse transcriptase (Cat#: PR-A3802) purchased from Promega (Madison, WI, USA). The cDNAs were subjected to quantitative PCR (qPCR) using SsoFast EvaGreen Supermix (Cat#: 1725205) purchased from Bio-Rad (Hercules, CA, USA) according to the manufacturer's instructions. Triplicates of samples were run on default settings of Bio-Rad CFX96 Real-Time PCR Detection System. Cq values of genes of interest were normalized to housekeeping gene *ACTIN* expression. The primer sequences are listed in the key resources table. All conditions were performed triplicate.

Preparation of whole-cell lysates

Cells were harvested, washed with PBS, and lysed in RIPA buffer supplemented with 5 mmol/L EDTA, 1 mmol/L NaV, 10 mmol/L NaF, and 1X Halt Protease Inhibitor Cocktail (Cat#: 78430) purchased from ThermoFisher Scientific (Milton Park, UK). Protein concentration was determined Pierce Bradford Plus Protein Assay Kit (Cat#: 23236) purchased from ThermoFisher Scientific (Milton Park, UK).

Immunoblotting

Protein extracts were resolved by SDS-PAGE and indicated primary antibodies were used. IGFBP3 (SC-365936) and Alpha Tubulin (SC-5286) were purchased from Santa Cruz Biotechnology (Santa Cruz, CA, USA). Phospho-Histone H2A.X (Ser139) (Cat#: 9718), Cleaved PARP (Cat#: 9541), Phospho-DNA-PKcs (Ser2056) (Cat#: 68716), Phospho-EGF Receptor (Tyr1068) (Cat#: 2234), EGF Receptor (Cat#: 4267), and DNA-PKcs (Cat#: 4602) were purchased from Cell Signaling Technology (Danvers, MA, USA). Anti-Rabbit (Cat#: NC0161557) and Anti-Mouse (Cat#: NC9575145) were purchased from ThermoFisher Scientific (Milton Park, UK). Alpha Tubulin was used as a control to monitor the amounts of samples applied. Proteins were visualized with Immobilon Crescendo Western HRP substrate (Cat#: WBLUR0500) purchased from Millipore (Burlington, MA, USA) using a Bio-Rad ChemiDoc MP Imaging System. All conditions were performed triplicate.

Enzyme-linked immunosorbent assay

The Human IGFBP3 Enzyme-Linked Immunosorbent Assay (ELISA) kit (Cat#: RAB0235) is an *in vitro* enzyme-linked immunosorbent assay for the quantitative measurement of human IGFBP-3 in serum, plasma, cell culture supernatants and urine purchased from Sigma-Aldrich. Culture supernatants were harvested and analyzed for IGFBP3 production by ELISA sandwich assay procedure. Samples and standards were assayed in duplicate according to the manufacturer's protocol. The EGFR (Phospho) [pY1068] Human ELISA Kit (Cat#: KHR9081) is a solid-phase sandwich ELISA designed to detect and quantify the level of EGFR (Phospho) [pY1068]) in fresh or frozen human cell lysates. Fresh cell lysates were harvested and analyzed for EGFR (Phospho) [pY1068]) production following the manufacturer's protocol. Samples and standards were assayed in duplicate according to the manufacturer's protocol. All conditions were performed triplicate.

QUANTIFICATION AND STATISTICAL ANALYSIS

All quantitated data are displayed as a percentage of control mean ± standard deviation. Data analysis was performed using GraphPad Prism 10.0 software. Statistical analyses were performed using the unpaired two-sided Student's *t* test, one-way or two-way ANOVA with a post hoc Tukey's honest significant difference (HSD) test when comparing at least three conditions. p-values of less than 0.05 were considered as statistically significant (*$p < 0.05$, **$p < 0.01$, ***$p < 0.001$). All experiments were repeated at least three times.